

Free-Standing Silver Nanocube/Graphene Oxide Hybrid Paper for Surface-Enhanced Raman Scattering

Wei Fan,^a Miao Yue-E,^a Xingyi Ling,^{a,b} and Tianxi Liu^{a,c}

^a State Key Laboratory of Modification of Chemical Fibers and Polymer Materials, College of Materials Science and Engineering, Donghua University, Shanghai 201620, China

^b Division of Chemistry and Biological Chemistry, School of Physical and Mathematical Sciences, Nanyang Technological University, 21 Nanyang Link, Singapore 637371, Singapore

^c State Key Laboratory of Molecular Engineering of Polymers, Department of Macromolecular Science, Fudan University, Shanghai 200433, China

Surface-enhanced Raman spectroscopy (SERS) as a powerful analytical tool has gained extensive attention. Despite of many efforts in the design of SERS substrates, it remains a great challenge for creating a universal substrate with long-term stability and reproducible SERS signals. In this work, Ag nanocubes and graphene oxide (GO) suspension were mixed to form a stable solution and further vacuum filtrated to obtain a free-standing hybrid paper. The Ag/GO hybrid papers exhibit excellent SERS activity because of the synergistic effect of Ag nanocubes and GO sheets. GO sheets can act as both SERS enhancement substrate and framework for supporting Ag nanocubes. Moreover, GO sheets can protect Ag nanoparticles from oxidation under ambient condition for prolonged life time SERS substrate. Furthermore, we demonstrate the use of the free-standing and flexible Ag/GO hybrid paper to enable direct, real-time and reliable detection of trace amounts of analytes in aqueous systems. This novel SERS substrate is expected to be applied in real-time analysis and expands the flexibility of SERS for useful applications in the materials and life science.

Keywords graphene, nanostructures, Ag nanocubes, free-standing, SERS enhancement

Introduction

Surface-enhanced Raman scattering (SERS) has attracted much attention because of high sensitivity for the analysis of various molecules at low concentrations, and has been widely demonstrated as a powerful analytical technique for ultra sensitive chemical or biochemical analyses.^[1-7] The impressive sensitivity of SERS over Raman spectroscopy stems from two enhancement mechanisms, namely electromagnetic and chemical enhancements. Electromagnetic mechanism is based on the enhancement of the local electromagnetic field (usually called hot-spots), which is mainly due to the excitation of localized surface plasmon resonances (LSPR) on the metal surface.^[8-11] Thus, the applications of SERS technique depend strongly on the LSPR properties of the nanostructured metal. Ag compared with other metals is the most promising, and indeed the most widely used material in plasmonics. It has been shown that localized electromagnetic fields are the most intense near regions with large radius of curvatures (sharp tips/edges) or having high asperities. In this regard, compared with sphere ones, other Ag architectures such

as nanocubes or octahedral give rise to stronger SERS signals.^[12,13] On the other hand, the chemical enhancement arises from the formation of a charge transfer complex that increases the polarizability of the molecule and produces an increase in the Raman scattering by 1 to 2 orders of magnitude.^[14-16]

Graphene, a single layer of sp^2 carbon network arranged in a perfect honeycomb lattice, has been extensively investigated because of its excellent mechanical and electrical properties.^[17-23] Besides the abundant theoretical and experimental interests in its electronic properties, graphene is also a rising star in SERS.^[24-26] Importantly, it has been shown that the most efficient chemical enhancement occurs for imperfect graphene, *i.e.* graphene possessing charge transfer groups. Thus, graphene oxide (GO), oxidized form of graphene, has become an ideal candidate for SRES substrate because of its distinct physical properties, which is derived from its unique chemical structure composed of segregated sp^2 carbon domains among sp^3 carbons presenting various oxygen containing functional groups.^[27] Chemical enhancement is thought to originate from the $\pi-\pi$ interactions and charge transfer from oxygen-rich functional

* E-mail: txliu@fudan.edu.cn, xyling@ntu.edu.sg; Tel.: 0086-021-55664197; Fax: 0086-021-65640293

Received December 22, 2015; accepted January 3, 2016; published online January 8, 2016.

Supporting information for this article is available on the WWW under <http://dx.doi.org/10.1002/cjoc.201500585> or from the author.

groups on GO.^[25] Mildly reduced GO has also been shown to lead to enhancement factors around 10³, implying that GO is a promising material for SERS applications.^[26]

Given the superior SERS capabilities of both metallic nanoparticles and graphene based materials, there are increasing studies focused on investigating the SERS efficiencies of composites of metallic nanoparticles and graphene. SERS signals arising from graphene/metal hybrid structures are also shown to have stronger SERS signals when compared to the individual component.^[28-37] Especially, SERS on Ag nanoparticle/GO hybrids has been investigated because of their amenable surface, large surface area, and high SERS activity. Several investigations have been carried out to synthesize Ag nanoparticle/GO hybrids both in solution phase^[36] and on solid substrates,^[37] indicating they are excellent candidates for SERS based sensors. However, among the extensive reports on the SERS capabilities of graphene-based metal nanoparticle hybrid materials, most of the Ag nanoparticles reported previously are spherical ones. Besides, the instability of Ag nanoparticles to oxidation under ambient condition still remains an important issue. Moreover, most of the substrates need external support such as silicon wafers, and a SERS substrate with a more flexible form and better universality is still lacking. The availability of a flexible substrate which can give stable and reproducible SERS response has remained a bottleneck for extending further applications of SERS.

In this study, we fabricated a free-standing and flexible SERS substrate with uniform, stable, reproducible and highly sensitive SERS signals. In our strategy, Ag nanocubes and GO suspension were mixed to form a stable solution and further vacuum filtrated to obtain a free-standing Ag nanocube/GO hybrid paper, which can be directly used as the SERS substrate without any external support. GO sheets can act as not only synergistic enhancement substrate, but also framework for supporting Ag nanocubes, as well as anti-oxidation sheath preventing Ag nanocubes from oxidation under ambient condition. Moreover, the formation of hot-spots between gapped Ag nanocubes will not be affected since GO sheets exhibit great permeability for the electromagnetic fields to pass through. This novel SERS substrate is expected to serve as flexible and high performance SERS platform, providing new opportunities for efficient chemical and biological sensing applications.

Experimental

Materials

Natural graphite powder (325 mesh) was purchased from Alfa-Aesar. Silver nitrate (AgNO₃, 99%), copper(II) chloride (CuCl₂), 3-amino-1-propanethiol (NH₂CH₂CH₂CH₂SH), 1,5-pentanediol and poly(vinyl pyrrolidone) (PVP, $M_w \approx 55000$ g/mol) were all ob-

tained from Sigma-Aldrich. Rhodamine 6G (R6G) from Sigma-Aldrich was used as Raman probes. All chemicals were used as received without further treatment. Deionized water (resistance > 18.0 MΩ•cm⁻¹) was used throughout all the experiments.

Synthesis of GO and Ag nanocubes

Graphite oxide was synthesized from natural graphite powder by a modified Hummers method.^[38] Exfoliation was carried out by sonicating 0.5 mg•mL⁻¹ graphite oxide dispersion under ambient condition for 30 min. The resulted homogeneous dispersion (GO) colored yellow-brown was diluted to 0.05 mg•mL⁻¹ for further use.

Silver nanocubes were synthesized according to a method as reported previously.^[39] In brief, silver nitrate (0.20 g) and copper(II) chloride (0.08 mg) were prepared separately in 10 mL 1,5-pentanediol. The chemicals were sonicated and vortexed repeatedly to dissolve them. 35 μL CuCl₂ solution was then added to AgNO₃ solution. In a separate vial, PVP (0.20 g) was dissolved in 1,5-pentanediol (10 mL). All solutions were dissolved using ultrasonic baths. Using a temperature-controlled silicone oil bath, 1,5-pentanediol (20 mL) was heated for 10 min in a 190 °C oil bath. The two precursor solutions were then injected into the hot reaction flask at the following rates: 500 μL of the silver nitrate solution every minute and 250 μL of the PVP solution every 30 s. This addition was stopped once the solution turned to opaque (in about 20 min). The product was purified by repeated filtration and washing with ethanol, and redispersed in ethanol for further use. Amino-modified Ag nanocubes were prepared by exchanging PVP with 3-amino-1-propanethiol in a 10 mmol/L ethanol solution, which was stirred for 12 h at room temperature under a stream of nitrogen to minimize oxidation. After repeatedly centrifuging and washing with ethanol and water, amino-modified Ag nanocubes were redispersed to 0.05 mg•mL⁻¹ in DI water under sonication for 0.5 h.

Fabrication of Ag nanocube/GO hybrid papers

A designed amount of Ag nanocube suspension (0.05 mg•mL⁻¹) was added to GO suspension drop by drop, and the resulting mixture was sonicated for another 2 h. Subsequently, the mixed suspension containing Ag nanocubes and GO was vacuum-filtrated through a PVDF membrane filter (220 nm pore size, Durapore® from Sigma-Aldrich). The weight ratios of Ag nanocubes to GO varied to 4/1, 2/1, 1/1 and 1/2, respectively, while the total weight was kept constant. To obtain a free-standing hybrid paper, the paper was dried at room temperature, and then carefully peeled off from the membrane filter. For comparison, neat GO paper was also fabricated in a similar way. To simplify, the fabricated Ag nanocube/GO hybrid papers with different weight ratios were denoted as AG41, AG21, AG11 and AG12, respectively.

Characterization

Field emission scanning electron microscopy (FE-SEM) characterization was conducted with a JSM-7600F SEM at an accelerating voltage of 5 kV. Transmission electron microscopy (TEM) observation was performed with a JEOL 2100 TEM under an accelerating voltage of 200 kV. Tapping mode atomic force microscopy (AFM) images were taken using a scanning probe microscope Nanoscope IV (Digital Instruments). The surface charge of the oppositely charged GO sheets synthesized was measured using a ζ -potential analyzer (Malvern, Zetasizer Nano ZS). X-ray photoelectron spectroscopy (XPS) spectra were measured using a Phoibos 100 spectrometer with a monochromatic Mg X-ray radiation source. All XPS spectra were fit using XPS Peak 4.1 software. Raman spectroscopy was obtained by the Raman touch microspectrometer (Nanophoton Inc, Osaka, Japan). All experiments were carried out with a $100\times$ objective lens ($NA=0.9$) and taken using 10 s acquisition time between 127 and 2672 cm^{-1} with an excitation wavelength of 532 nm. For all the SERS spectra presented here, each spectrum is the average of ten SERS spectra and has undergone baseline subtraction.

Results and Discussion

GO sheets and Ag nanocubes were separately prepared for this study. GO sheets were prepared using a modified Hummer's method,^[38] in which graphite oxide was subjected to chemical exfoliation and ultrasonication. The as-obtained GO sheets are rich in oxygen-rich functional groups, including epoxy, hydroxyl (OH^-) and carboxyl (COO^-) moieties.^[40] These oxygen-rich functional groups impart a negative charge to the GO sheets, with a ζ -potential of the aqueous suspension of GO sheets measured to be -45 mV . The morphology of GO is further characterized by atomic force microscopy (AFM). AFM image of the GO sheets (Figure 1a, b) clearly illustrates a perfect platelet structure with a thickness of about 1 nm and the lateral size is in a range of several dozens to hundreds of nanometers. Separately, Ag nanocubes were synthesized via a polyol reduction method, using 1,5-pentanediol as solvent at near-reflux temperature in the presence of poly(vinylpyrrolidone) (PVP) as a stabilizing agent.^[32] As shown in Figure 1c, the as-prepared Ag nanocubes are highly monodisperse, with average edge lengths of $121\pm 7\text{ nm}$. Amino-modified Ag nanocubes were further prepared by exchanging PVP with 3-amino-1-propanethiol, since the amino groups can form stronger electrostatic interactions with GO sheets and can form much more stable suspensions in water. These amino-modified Ag nanocubes were determined to be positively charged in aqueous solution, with a ζ -potential measured to be $+33\text{ mV}$.

In this study, a homogeneous suspension of Ag/GO hybrid was prepared by a direct self-assembly method, which is schematically illustrated in Figure 2a. Figure 2

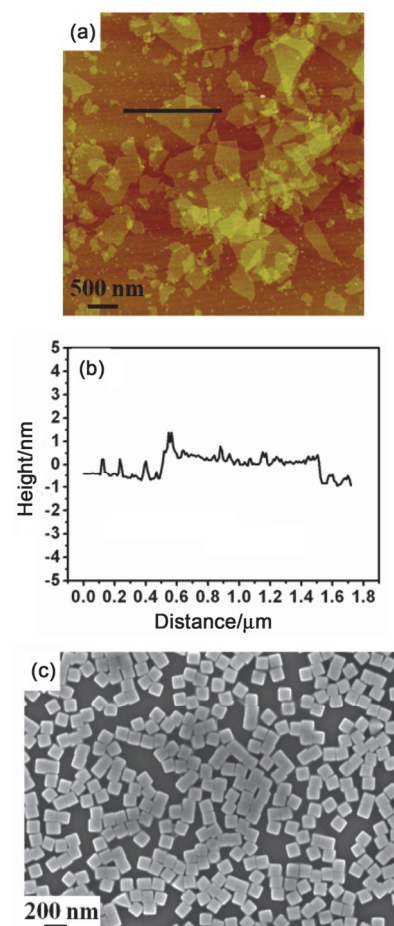


Figure 1 (a) AFM image of GO, (b) corresponding height profile, and (c) SEM image of Ag nanocubes.

illustrates the dispersibility of GO, amino-modified Ag nanocubes and Ag/GO (2/1, *w/w*) hybrid after settling for two weeks. The stability of the as-obtained GO sheet and amino-modified Ag nanocube dispersion is pretty good. For the case of Ag/GO (2/1, *w/w*) hybrid, no precipitation and stratification are observed at the bottom of the vial, as shown in Figure 2d. Through these, it can be concluded that GO sheets may act as unique two-dimensional (2D) dispersants for homogeneously dispersing Ag nanocubes in water, indicating strong electrostatic interactions between negatively charged GO sheets and positively charged amino-modified Ag nanocubes inside the hybrids.^[41,42] Direct evidence for the effective hybridization of Ag nanocubes with GO sheets can be obtained by TEM observations (Figure S1). As shown in Figure S1a, the GO sheets clearly illustrate a flake-like shape with some wrinkled and folded sheet structures at the edge. For Ag/GO hybrids, the Ag nanocubes are evenly anchored on both sides of 2D GO sheets, which help to prevent Ag nanocubes from agglomeration and enable a good dispersion of Ag nanocubes over its support, as shown in Figure S1b. Similarly, the presence of Ag nanocubes also greatly prevents the restacking or agglomeration of GO sheets. However, with the increase of Ag nanocube amount,

much more Ag nanocubes can be observed on GO sheets and some Ag aggregates are formed on the GO sheets, which are favorable for the formation of hot-spots between adjacent Ag nanocubes. Meanwhile, the arrangement of Ag nanocubes on GO sheets is observed to be not very close. Therefore, there are still some spaces between Ag nanocubes for the enrichment of the Raman probes in the procedure of SERS detection.

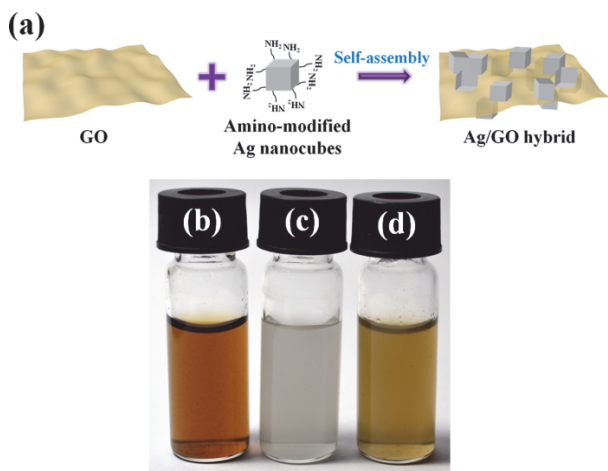
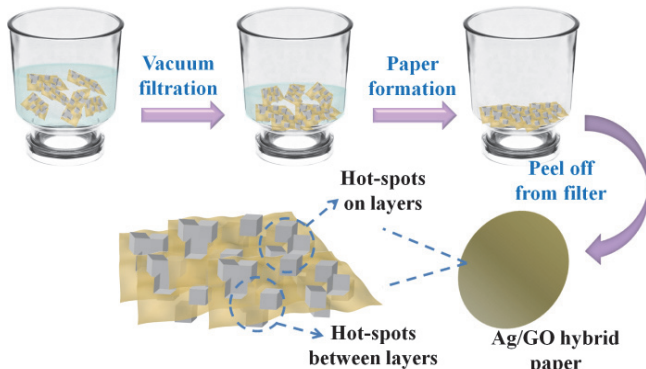


Figure 2 (a) Schematic illustration for the self-assembly of GO sheets and amino-modified Ag nanocubes. Digital images showing the dispersion of (b) GO, (c) amino-modified Ag nanocubes, and (d) Ag/GO 2-1 hybrid in water. The image shows the dispersions after settling for two weeks.

Vacuum filtration of stable GO and Ag/GO hybrid dispersions through a membrane filter can form uniform films. The thickness of the film can be adjusted from dozen of nanometers to tens of micrometers by changing the volume and concentration of dispersion.^[43-46] The fabrication of Ag/GO hybrid papers with Ag nanocubes parallel arranged graphene frameworks is illustrated in Scheme 1. Neat GO sheets were also vacuum filtrated in a similar way. As shown in Scheme 1, a homogeneous dispersion of Ag/GO hybrids was vacuum filtrated onto a filter, with a preferential plane orienta-

Scheme 1 Schematic illustration for the fabrication of free-standing Ag/GO hybrid papers and possible mechanism for the formation of hot-spots



tion of 2D GO sheets due to vacuum pressure upon filtration. A paper-like film adhering on the filter was then obtained, and the thickness of the resultant film can be easily tailored by varying the volume of dispersions for filtration. As seen from the digital photos in Figure S2, Ag/GO hybrid papers are adhered to the filters in a good condition. After dried at room temperature, free-standing GO and Ag/GO hybrid papers can be easily peeled off from the filter. However, when further increasing the weight ratio of Ag nanocubes (*e.g.* AG41), it becomes too brittle to form a paper-like film (Figure S2c).

In order to investigate microscopic morphologies of these papers, SEM observation was carried out on both surfaces and cross-sections of neat GO and Ag/GO hybrid papers, as shown in Figure 3 and Figure 4, respectively. Neat GO paper exhibits a rough surface with the edges of some GO sheets wrinkled and tilted up. For Ag/GO hybrid papers, it can be clearly observed that large amounts of silver nanoparticles with diameter of *ca.* 120 nm are uniformly embedded in GO sheets, which is consistent with the TEM observations (Figure S1). Although the surface of Ag/GO hybrid papers is much rougher than that of the GO paper, the Ag/GO hybrid paper displays better reflectivity and luster, which is due to the content of Ag nanocubes in film. The photograph in Figure S2b shows that the film obtained from filtration is shiny luster with good flexibility and tough enough to be folded. With the increase of Ag nanocube content, the number of Ag nanocubes increases obviously. For AG21 paper, some aggregates of Ag nanocubes are formed on the paper surface, which are favourable for the formation of hot-spots between adjacent Ag nanocubes, and may further enhance the SERS signals.

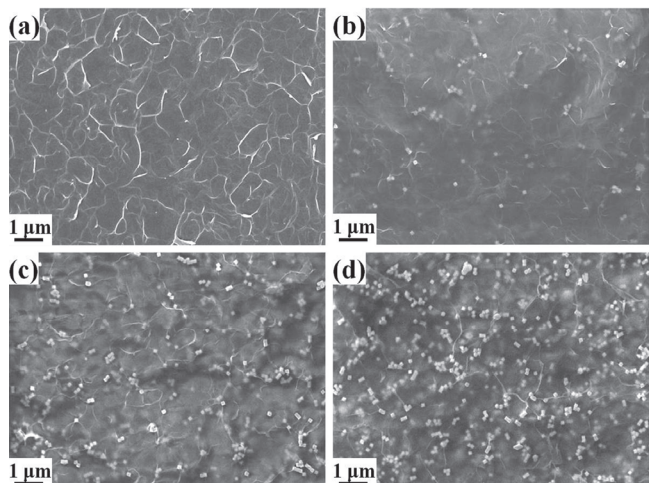


Figure 3 SEM images of the surfaces of (a) GO, (b) AG12, (c) AG11, and (d) AG21 papers.

Figure 4 shows the fractured edges of neat GO and Ag/GO hybrid papers. The thickness of these papers was in a range of approximately 1–2 μm, and the thickness slightly decreased with the decrease of GO amount.

It should be noticed that the hybrid papers used as SERS substrate should be thin enough for the laser to penetrate through. Here, the thickness of the hybrid paper was optimized just enough for forming a free-standing paper (that is, with a good film-forming ability). All the neat GO and hybrid papers clearly exhibit a well-packed layered structure through the entire cross-sections, indicating that GO and Ag/GO hybrids can be assembled to form parallel arranged nanostructures under filtration-induced directional flow. Ag nanocubes are incorporated between large lateral dimensional GO layers, resulting in sandwiched structures, and there are irregular pores between Ag nanocubes and GO sheets. At a low content of Ag nanocubes (e.g. AG11 and AG12 papers), GO sheets and Ag nanocubes are closely packed in the lateral direction and form continuous frameworks, which is partially attributed to self-assembly behavior of GO sheets and Ag nanocubes during the filtration process. Nevertheless, for the case of AG21 paper, slight aggregation of Ag nanocubes was observed in the space between the parallel arranged GO frameworks (Figure 4d and 4h), which can also form hot-spots between different GO layers. Therefore, this unique sandwiched structure largely increases the density of hot-spots for SERS enhancement.

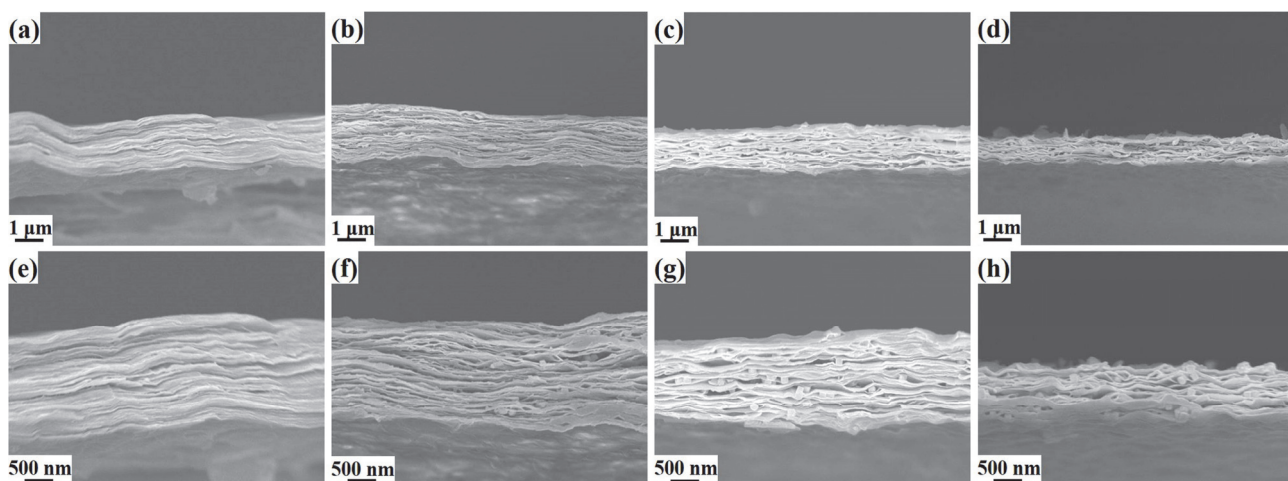


Figure 4 SEM images of the cross-sections of (a) GO, (b) AG12, (c) AG11, and (d) AG21 papers. (e–h) show the corresponding images at high magnifications.

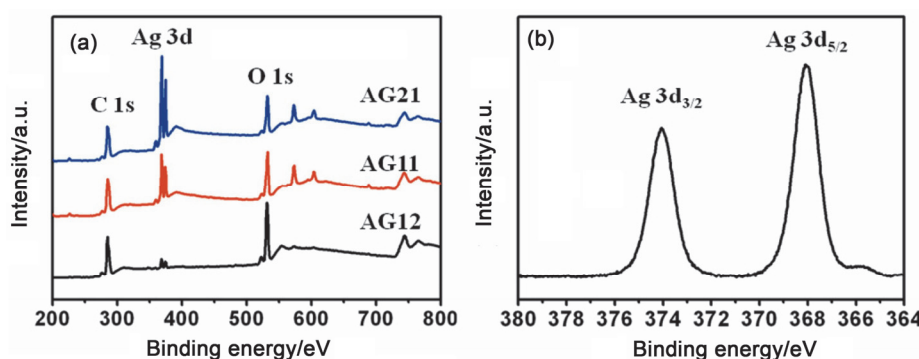


Figure 5 (a) XPS spectra of AG12, AG11, and AG21 papers. (b) High resolution Ag 3d spectrum of AG21 paper.

Figure 5 shows the XPS spectra of the as-prepared AG12, AG11 and AG21 papers. The survey scan (Figure 5a) shows the presence of silver, carbon, oxygen elements in the sample with no detectable impurities being observed. The peak area corresponding to Ag 3d increases gradually from AG12 to AG21 samples, indicating the increase of silver atom percentage, which is in accordance with the weight ratio of Ag nanocubes. Furthermore, the high-resolution XPS spectrum of Ag 3d region (Figure 5b) consists of a spin-orbit coupling doublet with binding energy of 368.1 eV for Ag 3d_{5/2} state and 374.1 eV for Ag 3d_{3/2} state, which correspond to Ag⁰ state.^[47]

These free-standing GO and Ag/GO hybrid papers exhibit SERS activity and can be directly used as SERS substrates without any external support such as silicon wafer. Aromatic molecules, rhodamine 6G (R6G) is selected as the probe molecule since it possesses well-defined molecular fingerprints in their Raman spectra and is commonly employed as probes for evaluating the sensing capabilities of various systems.^[48,49] Figure 6 shows the representative Raman spectra of R6G on GO, AG12, AG11 and AG21 papers after immersion of each substrate in 10⁻⁶ mol/L aqueous R6G solution for 2 h to induce surface adsorption. Since the typical D and

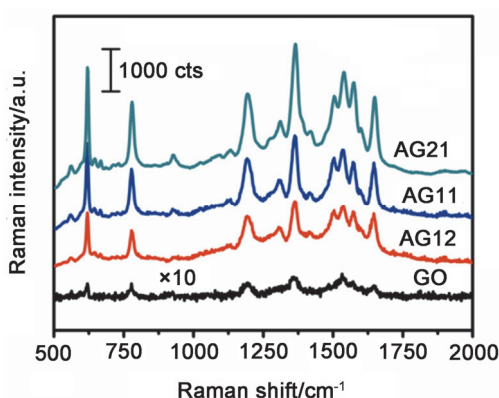


Figure 6 SERS spectra of 10^{-6} mol/L R6G obtained on GO, AG12, AG11, and AG21 papers. Each spectrum is the average of ten SERS spectra and has undergone baseline subtraction.

G bands of GO overlap with the Raman signal of R6G, the SERS spectra of R6G are normalized here by subtracting the signals of the corresponding papers (Figure S3). Raman spectrum of R6G on GO paper exhibits relatively low enhancement which is mainly due to the chemical enhancement.^[50] Nevertheless, notable Raman signal enhancement of R6G is observed for Ag/GO hybrid papers. The SERS intensity of R6G on Ag/GO hybrid papers is increased by thirty- to one hundred-fold with the increase of silver nanoparticle content in the hybrid papers in comparison to that on bare GO paper. The remarkable enhancement of SERS signals obtained for Ag/GO hybrid papers can be explained as follows. Firstly, Ag nanocubes give rise to stronger SERS signals compared to spherical particles. This is attributed to more intense local electromagnetic fields generated around the sharp edges/vertices of the nanocubes. Secondly, with the increase of Ag nanocube content, some aggregates of Ag nanocubes can be formed on GO sheets. Thus, the electromagnetic hot-spots (which are the origin of a huge SERS enhancement) can be created by the coupling of localized surface plasmon resonance between gapped metal nanoparticles. As illustrated in Scheme 1, the hot-spots can be formed not only on the same GO sheets, but also between the adjacent GO sheets since GO exhibits good permeability for the electromagnetic hot spots to pass through.^[28] Finally, charge-transfer complexes can be formed between Ag nanocubes and GO sheets. These complexes can absorb light at excitation frequency to produce chemical SERS effect. The degree of enhancement can be tuned by changing the density of Ag nanocubes in the hybrid papers. The contact area between Ag nanocubes and GO sheets increases with the increase of Ag nanocube content in the hybrid papers. The increase of contact area leads to an increase of charge-transfer complexes which are responsible for the chemical enhancement in SERS.

The adsorption kinetics of R6G was examined by measuring the changes of relative intensity of SERS signal on Ag/GO hybrid papers as a function of immersing time (Figure 7a). The AG21 paper was im-

mersed in 10^{-6} mol/L aqueous R6G solution for 30 min, 60 min, 90 min, 120 min, 150 min and 180 min, respectively. SERS signal of R6G on AG21 paper increased gradually with incubation time and almost saturated after 120 min (Figure 7b). As shown in Figure S4, the UV-visible absorbance of 10^{-6} mol/L R6G solution after the adsorption by Ag nanocubes is much higher than that of the solution after the adsorption by AG21 paper containing the same amount of Ag nanocubes. According to this figure, in this case, the amount of R6G adsorbed by AG21 paper is about 6 times that adsorbed by Agnanocubes. This result indicated that the presence of GO sheets in the hybrid paper accelerated the adsorption of R6G due to the strong π - π interaction between them.^[30,51] The detection limits and linearity range of the SERS sensing of Ag/GO hybrid paper are also studied (Figure 7c, 7d). The detection limit for R6G is monitored using 621 cm^{-1} and 1193 cm^{-1} bands, and SERS signals (with signal/noise ratio >3) can still be detected down to 10^{-10} mol/L (Figure 7c). This low detection limit may be due to the increased adsorption force, both physically and chemically between aromatic molecules and GO sheets, especially at low concentrations.^[24] Both the enrichment effect of molecules and their chemical interactions with GO sheets should be taken into consideration.^[52] The linearity range spans across 5 orders of magnitude, from 10^{-10} to 10^{-6} mol/L. The detection limit for CV (Figure S5) is also investigated and is down to 10^{-9} mol/L, which is monitored using the vibrational modes at 1178 and 918 cm^{-1} . The detection limits obtained using both R6G and CV as Raman probe in our experiment are comparable to the ones reported in the literature.^[53,54]

It is well known that Ag nanoparticles will undergo irreversible oxidation when exposed in air. To investigate the stability of Ag/GO hybrid papers as SERS substrate, the AG21 paper was exposed to ambient condition for designated durations of 0, 3, and 7 d. Then, the AG21 papers stored for different days were respectively incubated in 10^{-6} mol/L R6G aqueous solution for 2 h and finally analyzed by Raman spectroscopy. For comparison, Ag nanocube films on silicon substrate were fabricated by Langmuir-Blodgett (LB) method, and the corresponding SEM images are shown in Figure S6. SERS spectra of R6G on AG21 papers and Ag nanocube LB films are shown in Figure 8a and 8b, respectively. SERS intensities at 621 cm^{-1} derived from xanthene ring deformation modes of R6G on AG21 papers and Ag nanocube LB films are also obtained (Figure 8c). The SERS intensity of R6G on AG21 paper is lower than that on the freshly prepared Ag nanocube LB film, which is mainly due to the relatively low content of Ag nanocubes. However, after Ag nanocube LB films are exposed to ambient condition for 3 and 7 d, the relative intensity of SERS signal for R6G significantly decreases by 39% and 74%, respectively. By contrast, SERS intensity of R6G obtained on AG21 paper almost remains the same after 7 d exposure. This result indi-

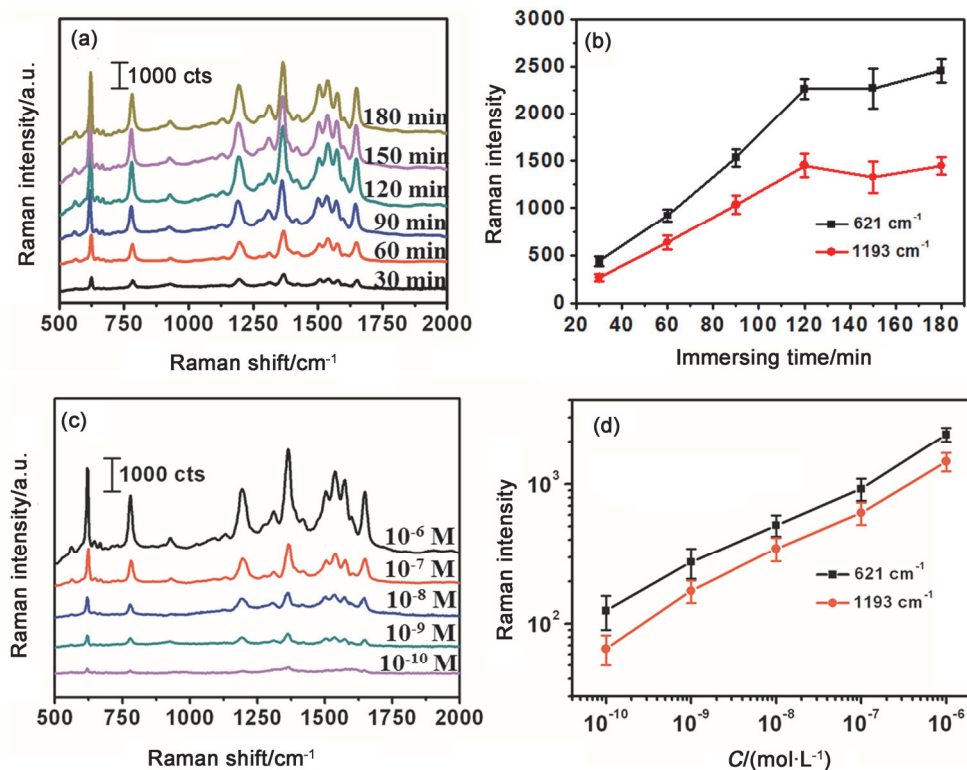


Figure 7 (a) SERS spectra of R6G obtained on AG21 paper with varying immersing time for adsorption in 10⁻⁶ mol/L aqueous R6G. (b) A plot of SERS signal intensities of R6G at 621 and 1193 cm⁻¹ on AG21 paper versus immersing time. (c) SERS spectra of R6G on AG21 paper by soaking in the solution with different concentrations labeled in the respective SERS spectra. (d) The corresponding plots of SERS signal intensity versus concentration of R6G.

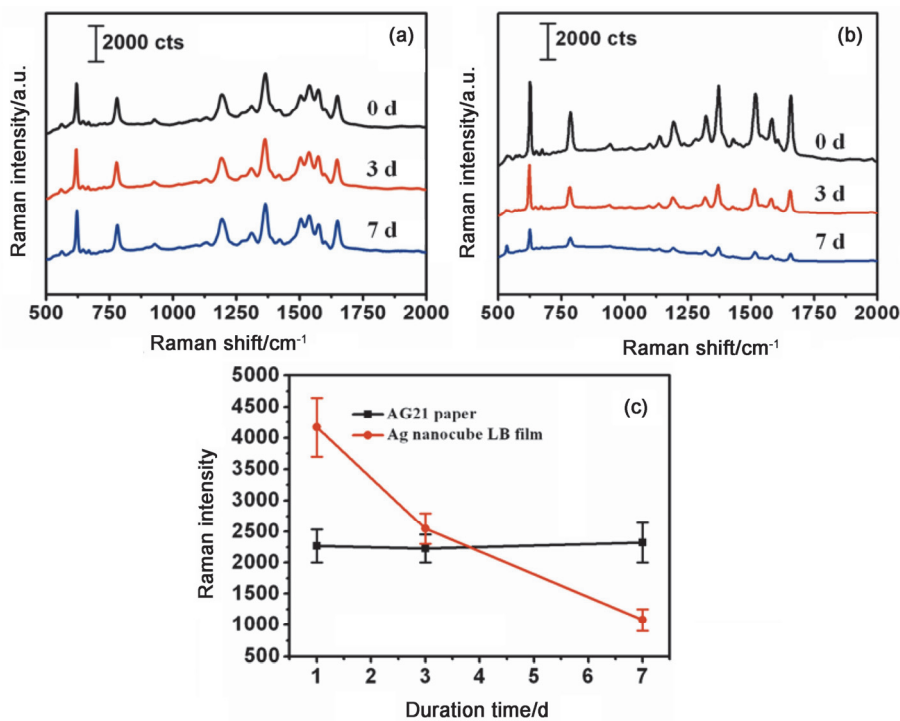


Figure 8 SERS spectra of R6G obtained on (a) AG21 paper and (b) Ag nanocube LB film after exposure to ambient condition for 0, 3, and 7 d. (c) The plots of SERS signal intensity at 621 cm⁻¹ on AG21 paper and Ag nanocube LB film.

cates that SERS signal on Ag/GO hybrid papers is much more stable even after exposure to ambient condition

compared to that on Ag nanocube LB films. Morphological changes of AG21 paper and Ag nanocubes after

exposure to ambient condition are observed by SEM images as shown in Figure S7. Almost no difference is observed for AG21 paper while small particles appear on the surface of Ag nanocubes after exposure. This can be attributed to the presence of GO sheets which protect Ag nanocubes from oxidation. Although some Ag nanocubes do exist on the surface of the hybrid papers, most of Ag nanocubes are embedded between GO layers, and thus Ag nanocubes are protected from direct contacting with air. Therefore, Ag/GO hybrid papers show excellent stability as sustained SERS substrates.

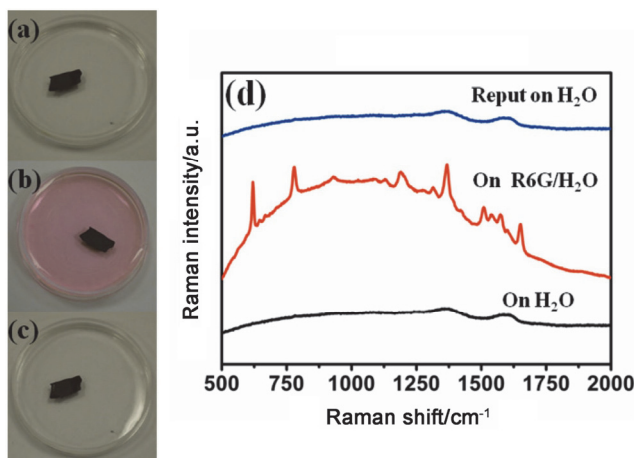


Figure 9 A real-time and reversible detection of R6G by placing AG21 paper directly on the surface of 10^{-6} mol/L R6G aqueous solution. (a–c) Digital photos and (d) Raman spectra of the same AG21 paper on H_2O , R6G/ H_2O and reput on H_2O , respectively.

A “universal” substrate should be sufficiently economical, convenient, and compatible with various samples in different states. Such free-standing and flexible Ag/GO hybrid papers do not require special sample preparation, and are very convenient for in-situ characterization or real-time monitoring. As shown in Figure 9, Ag/GO hybrid papers can be used directly for real-time analysis of samples in an aqueous solution, where such AG21 paper was first put floating on water, and a clean baseline was obtained with a clear GO signal. Then, the same AG21 paper was placed on the surface of a 1×10^{-6} mol/L aqueous solution of R6G, and the intrinsic signal of R6G appeared in the Raman spectra. The broad background peak is due to the fluorescence of R6G. Finally, the R6G signal disappeared after washing and placing AG21 paper on water back again. This good reversibility suggests that AG21 paper may be exploited in real-time sensing processes, such as online monitoring of water contaminants. Therefore, this novel kind of free-standing and flexible SERS substrate is expected to be widely used for direct, noninvasive and ultrasensitive Raman measurements, including real-time monitoring on solution surfaces or other surfaces with any arbitrary morphology.

Conclusions

In summary, free-standing and flexible Ag nanocube/GO hybrid papers have been fabricated successfully via a simple and convenient vacuum filtration method. The Ag/GO hybrid papers exhibit excellent SERS activity due to the synergistic effect of Ag nanocubes and GO sheets, and the SERS signals can be optimized by simply tuning the composition of Ag/GO hybrids. The hybrid paper shows fast adsorption kinetics toward R6G, a model Raman probe molecule, with a low detection limit of 10^{-10} mol/L. Furthermore, Ag/GO hybrid papers can effectively protect Ag nanocubes from oxidation under ambient condition for prolonged time up to several weeks with reproducible SERS signals. Therefore, the free-standing and flexible Ag nanocube/GO hybrid paper is sufficiently economical, convenient, and compatible with various samples in different states, which may find potential applications in real-time sensing.

Acknowledgement

The authors are grateful for the financial support from the National Natural Science Foundation of China (Nos. 51125011, 51433001), and the National Research Foundation, Singapore (No. NRF-NRFF2012-04), Nanyang Technological University's start-up grant.

References

- [1] Nie, S. M.; Emery, S. R. *Science* **1997**, *275*, 1102.
- [2] Stewart, M. E.; Anderton, C. R.; Thompson, L. B.; Maria, J. S.; Gray, K.; Rogers, J. A.; Nuzzo, R. G. *Chem. Rev.* **2008**, *108*, 494.
- [3] Sharma, B.; Frontiera, R. R.; Henry, A. I.; Ringe, E.; Duyne, R. P. V. *Mater. Today* **2012**, *15*, 16.
- [4] Ko, H.; Singamaneni, S.; Tsukruk, V. V. *Small* **2008**, *4*, 1576.
- [5] Wu, D. Y.; Liu, X. M.; Duan, S.; Xu, X.; Ren, B.; Lin, S. H.; Tian, Z. *Q. J. Phys. Chem. C* **2008**, *112*, 4195.
- [6] Lecomte, S.; Matejka, P.; Baron, M. H. *Langmuir* **1998**, *14*, 4373.
- [7] Doering, W. E.; Nie, S. M. *J. Phys. Chem. B* **2002**, *106*, 311.
- [8] Willets, K. A.; Duyne, R. P. V. *Annu. Rev. Phys. Chem.* **2007**, *58*, 267.
- [9] Zhao, J.; Pinchuk, A. O.; McMahon, J. M.; Li, S. Z.; Ausman, L. K.; Atkinson, A. L.; Schatz, G. C. *Acc. Chem. Res.* **2008**, *41*, 1710.
- [10] Rycenga, M.; Cobley, C. M.; Zeng, J.; Li, W. Y.; Moran, C. H.; Zhang, Q.; Qin, D.; Xia, Y. N. *Chem. Rev.* **2011**, *111*, 3669.
- [11] Rodriguez-Lorenzo, L.; Alvarez-Puebla, R. A.; Pastoriza-Santos, I.; Mazzucco, S.; Stephan, O.; Kociak, M.; Liz-Marzan, L. M.; Abajo, F. J. *G. J. Am. Chem. Soc.* **2009**, *131*, 4616.
- [12] Wang, X. S.; Huang, P.; Feng, L. L.; He, M.; Guo, S. W.; Shen, G. X.; Cui, D. X. *RSC Adv.* **2012**, *2*, 3816.
- [13] Fan, W.; Lee, Y. H.; Pedireddy, S.; Zhang, Q.; Liu, T. X.; Ling, X. Y. *Nanoscale* **2014**, *6*, 4843.
- [14] Yang, Y.; Matsubara, S.; Xiong, L. M.; Hayakawa, T.; Nogami, M. *J. Phys. Chem. C* **2007**, *111*, 9095.
- [15] Rycenga, M.; Camargo, P.; Li, W. Y.; Moran, C. H.; Xia, Y. N. *J. Phys. Chem. Lett.* **2010**, *1*, 696.
- [16] Kelly, K. L.; Coronado, E.; Zhao, L. L.; Schatz, G. C. *J. Phys. Chem. B* **2003**, *107*, 668.
- [17] Novoselov, K. S.; Geim, A. K.; Morozov, S. V.; Jiang, D.; Zhang, Y.; Dubonos, S. V.; Grigorieva, I. V.; Firsov, A. A. *Science* **2004**, *306*,

666.

- [18] Rao, C. N. R.; Sood, A. K.; Subrahmanyam, K. S.; Govindaraj, A. *Angew. Chem., Int. Ed.* **2009**, *48*, 7752.
- [19] Zhang, Y. B.; Tan, Y. W.; Stormer, H. L.; Kim, P. *Nature* **2005**, *438*, 201.
- [20] Wang, J. C.; Wang, X. B.; Wan, L.; Yang, Y. K.; Wang, S. M. *Chin. J. Chem.* **2010**, *28*, 1935.
- [21] Li, L.; Hu, Z. G.; Yang, Y. Y.; Liang, P. J.; Lu, A. L.; Xu, H.; Hu, Y. Y.; Wu, H. Y. *Chin. J. Chem.* **2013**, *31*, 1290.
- [22] Wang, L. P.; Liu, M. L.; Meng, Y.; Li, H. T.; Zhang, Y. Y.; Yao, S. Z. *Chin. J. Chem.* **2013**, *31*, 845.
- [23] Shi, M. Q.; Zhao, D.; Liu, W. M.; Chu, Y. Q.; Ma, C. A. *Chin. J. Chem.* **2014**, *32*, 233.
- [24] Xu, W. G.; Mao, N. N.; Zhang, J. *Small* **2013**, *9*, 1206.
- [25] Ling, X.; Moura, L. G.; Pimenta, M. A.; Zhang, J. *J. Phys. Chem. C* **2012**, *116*, 25112.
- [26] Yu, X. X.; Cai, H. B.; Zhang, W. H.; Li, X. J.; Pan, N.; Luo, Y.; Wang, X. P.; Hou, J. G. *ACS Nano* **2011**, *5*, 952.
- [27] Stankovich, S.; Dikin, D. A.; Piner, R. D.; Kohlhaas, K. A.; Kleinhammes, A.; Jia, Y.; Wu, Y.; Nguyen, S. T.; Ruoff, R. S. *Carbon* **2007**, *45*, 1558.
- [28] Xu, W. G.; Ling, X.; Xiao, J. Q.; Dresselhaus, M. S.; Kong, J.; Xu, H. X.; Liu, Z. F.; Zhang, J. *Proc. Natl. Acad. Sci. U. S. A.* **2012**, *109*, 9281.
- [29] Xu, W. G.; Xiao, J. Q.; Chen, Y. F.; Chen, Y. B.; Ling, X.; Zhang, J. *Adv. Mater.* **2013**, *25*, 928.
- [30] Liu, X. J.; Cao, L. Y.; Song, W.; Ai, K. L.; Lu, L. H. *ACS Appl. Mater. Interfaces* **2011**, *3*, 2944.
- [31] Huang, J.; Zhang, L. M.; Chen, B.; Ji, N.; Chen, F. H.; Zhang, Y.; Zhang, Z. *J. Nanoscale* **2010**, *2*, 2733.
- [32] Zhang, Z.; Xu, F. G.; Yang, W. S.; Guo, M. Y.; Wang, X. D.; Zhang, B. L.; Tang, J. L. *Chem. Commun.* **2011**, *47*, 6440.
- [33] Fu, X. Q.; Bei, F. L.; Wang, X.; O'Brien, S.; Lombardi, J. R. *Nanoscale* **2010**, *2*, 1461.
- [34] Dutta, S.; Ray, C.; Sarkar, S.; Pradhan, M.; Negishi, Y.; Pal, T. *Appl. Mater. Interfaces* **2013**, *5*, 8724.
- [35] Li, S. K.; Yan, Y. X.; Wang, J. L.; Yu, S. H. *Nanoscale* **2013**, *5*, 12616.
- [36] Tang, X. Z.; Cao, Z.; Zhang, H. B.; Liu, J.; Yu, Z. Z. *Chem. Commun.* **2011**, *47*, 3084.
- [37] Kim, Y. K.; Han, S. W.; Min, D. H. *ACS Appl. Mater. Interfaces* **2012**, *4*, 6545.
- [38] Kovtyukhova, N. I.; Ollivier, P. J.; Martin, B. R.; Mallouk, T. E.; Chizhik, S. A.; Buzaneva, E. V.; Gorchinskiy, A. D. *Chem. Mater.* **1999**, *11*, 771.
- [39] Tao, A.; Sinsermsuksakul, P.; Yang, P. D. *Angew. Chem., Int. Ed.* **2006**, *45*, 4597.
- [40] Dreyer, D. R.; Park, S.; Bielawski, C. W.; Ruoff, R. S. *Chem. Soc. Rev.* **2010**, *39*, 228.
- [41] Zhang, L. L.; Xiong, Z.; Zhao, X. S. *ACS Nano* **2010**, *4*, 7030.
- [42] Zhang, C.; Huang, S.; Tjiu, W. W.; Fan, W.; Liu, T. X. *J. Mater. Chem.* **2012**, *22*, 2427.
- [43] Dikin, D. A.; Stankovich, S.; Zimney, E. J.; Piner, R. D.; Domke, G. H. B.; Evmenenko, G.; Nguyen, S. T.; Ruoff, R. S. *Nature* **2007**, *448*, 457.
- [44] Xu, Z. X.; Gao, H. Y.; Hu, G. X. *Carbon* **2011**, *49*, 4731.
- [45] Liu, Y.; Wang, W.; Gu, L.; Wang, Y. W.; Ying, Y. L.; Mao, Y. Y.; Sun, L. W.; Peng, X. S. *ACS Appl. Mater. Interfaces* **2013**, *5*, 9850.
- [46] Tan, Y. Q.; Song, Y. H.; Zheng, Q. *Chin. J. Polym. Sci.* **2013**, *31*, 399.
- [47] Lu, Z.; Cheng, H.; Lo, M.; Chung, C. Y. *Adv. Funct. Mater.* **2007**, *17*, 3885.
- [48] Mulvihill, M.; Tao, A.; Benjauthrit, K.; Arnold, J.; Yang, P. *Angew. Chem., Int. Ed.* **2008**, *47*, 6456.
- [49] Kim, A.; Barcelo, S. J.; Williams, R. S.; Li, Z. Y. *Anal. Chem.* **2012**, *84*, 9303.
- [50] Ling, X.; Moura, L. G.; Pimenta, M. A.; Zhang, J. *J. Phys. Chem. C* **2012**, *116*, 25112.
- [51] Luo, P. H.; Li, C.; Shi, G. Q. *Phys. Chem. Chem. Phys.* **2012**, *14*, 7360.
- [52] Kong, X. K.; Chen, Q. W. *J. Mater. Chem.* **2012**, *22*, 15336.
- [53] Galopin, E.; Barbillat, J.; Coffinier, Y.; Szunerits, S.; Patriarche, G.; Boukherroub, R. *ACS Appl. Mater. Interfaces* **2009**, *1*, 1396.
- [54] Liu, Y. C.; Yu, C. C.; Shen, S. F. *J. Mater. Chem.* **2006**, *16*, 3546.

(Cheng, F.)